A COMPLEX DATA METHOD TO COMPUTE FMRI ACTIVATION

Daniel B. Rowe

Department of Biophysics
Medical College of Wisconsin
8701 Watertown Plank Road
Milwaukee, WI 53226

ABSTRACT

In functional magnetic resonance imaging, voxel time courses after Fourier or non-Fourier "image reconstruction" are complex valued as a result of phase imperfections due to magnetic field inhomogeneities and random noise. Nearly all fMRI studies derive functional "activation" based on magnitude-only voxel time courses. Here the entire complex or bivariate data are modeled rather than just the magnitude-only data. A nonlinear multiple regression model is used to model activation of the complex signal, and a likelihood ratio test is derived to determine activation in each voxel. The magnitude-only and complex time course models are applied to a real dataset.

1. INTRODUCTION

In magnetic resonance imaging, after Fourier or non-Fourier image reconstruction, each voxel contains a time course of real and imaginary components. Magnitude-only images are produced by taking the square root of the sum of squares of the real and imaginary parts of the complex valued time courses in each voxel at each time point. Nearly all fMRI studies obtain a statistical measure of functional activation based on magnitude-only image time courses. When this is done, phase information in the data is discarded. This is illustrated in Fig. 1, where real-imaginary and magnitude-phase image sequences are shown to depict the example dataset discussed later.

Magnitude-only models [2, 4] typically assume normally distributed errors; alternatively, one can assume that the original real and imaginary components of the PSD have normally distributed errors. Independent normally distributed errors on the measured complex signal translates to a Ricean distributed [10] magnitude image that is approximately normal for large signal-to-noise ratios.

When computing magnitude-only image time courses and activations, the signal-to-noise ratio (SNR) may not be large enough for this approximate normality to hold. This is increasingly true with higher voxel resolutions and in areas with a large degree of signal dropout. In addition, phase information or half of the numbers are discarded. A more accurate model should properly model the noise and use all the information contained in the real and imaginary components of the data.

Previous models for complex fMRI data have been proposed, [7, 9]. The first by and Lai and Glover (1997) did not accurately model the phase, while here the phase is correctly accounted for through a nonlinear multiple regression model. The second model by Nan and Nowak (1999) correctly modeled the phase coupling between the means of the real and imaginary components, but was limited to a single baseline and signal model because of their model parameterization. In addition, the second model did not directly estimate the regression coefficients or phase angle and used critical values based on Monte Carlo simulation. The second model is reparameterized and extended to a multiparameter baseline and signal model. Additionally, hypothesis tests are formulated in terms of contrasts, which allows for more elaborate testing such as deconvolution and comparisons between multiple task conditions. Finally, the current parameterization allows the estimation of the phase angle directly instead of the sine and cosine of the phase angle. The results of the proposed model are compared to a strict magnitude-only model in terms of thresholded activation maps on a real dataset.

2. MODEL

In MRI/fMRI, the aim is to image a real valued physical object $\rho(x, y)$ and obtain a measured object $\rho_m(x, y)$ by measuring a 2D complex valued signal $s_m(k_x, k_y)$ at spatial frequencies (k_x, k_y). This signal consists of a true complex valued signal $s(k_x, k_y)$ plus a random complex noise term $\delta(k_x, k_y)$ with real and imaginary components that are assumed to be independent and identically normally distributed. Even if there were no phase imperfections, it is necessary to observe the imaginary parts of this signal because we phase encode for proper image formation. After image reconstruction, we obtain a complex valued measured object plus complex valued noise.

Fig. 1. Image sequences.

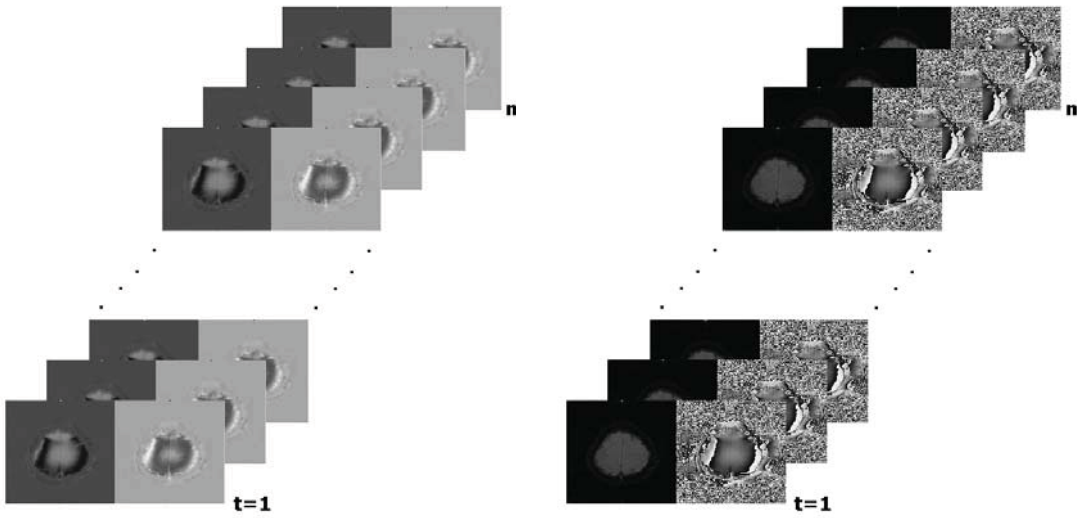

(a)Real-Imaginary (b)Magnitude-Phase

Fig. 2. Real Imaginary vector in a voxel over time.

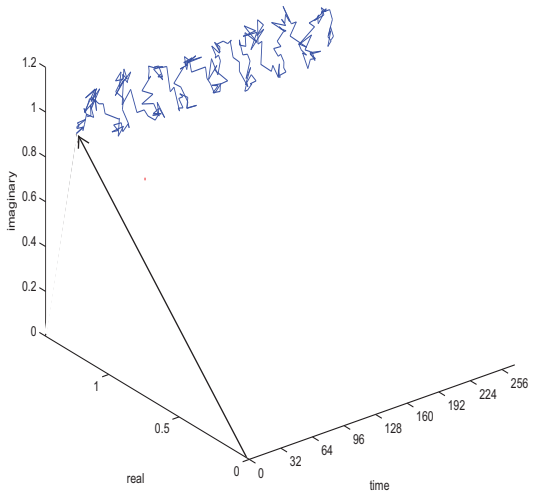

Neglecting the voxel location and focusing on a particular voxel, the complex valued image measured over time in a given voxel is

$$\rho_{mt} \quad = \quad [\rho_{Rt} + \eta_{Rt}] + i[\rho_{It} + \eta_{It}]$$

where $(\eta_{Rt}, \eta_{It})' \sim \mathcal{N}(0, \Sigma)$ and $\Sigma = \sigma^2 I_2$. The distributional specification is on the real and imaginary parts of the image and not on the magnitude.

A nonlinear multiple regression model is introduced individually for each voxel that includes a phase imperfection θ in which at time t, the measured effective proton spin density is given by

$$\rho_{mt} \quad = \quad [x_t'\beta \cos\theta + \eta_{Rt}] + i[x_t'\beta \sin\theta + \eta_{It}] \quad (1)$$

where $\rho_t = x_t'\beta = \beta_0 + \beta_1 x_{1t} + \cdots + \beta_q x_{qt}$. The phase imperfection in Eq. 1 is a fixed and unknown quantity, which may be estimated voxel by voxel.

In fMRI, we take repeated measurements over time while a subject is performing a task. In each voxel, we compute a measure of association between the observed time course and a preassigned reference function that characterizes the experimental paradigm.

2.1. Magnitude-Only Activation

The typical method to compute activations [2, 4] is to use only the magnitude which is denoted by y_t and written as

$$y_t = \left[(x_t'\beta \cos\theta + \eta_{Rt})^2 + (x_t'\beta \sin\theta + \eta_{It})^2\right]^{\frac{1}{2}}. \quad (2)$$

The magnitude-only model in Eq. 2 discards any information contained in the phase, given by

$$\phi_t \quad = \quad \tan^{-1}\left[\frac{\rho_{It} + \eta_{It}}{\rho_{Rt} + \eta_{Rt}}\right].$$

The magnitude is not normally distributed but is Ricean distributed. Both the magnitude and the phase are approximately normal for large SNR's [5, 10] as outlined in the appendix. The special case of the Ricean where there is no signal is known as the Rayleigh distribution. It is known

[6] that a histogram of noise outside the brain without any signal is Rayleigh distributed.

The Ricean distribution is approximately normal for large signal-to-noise ratios (small relative error variance). This can be shown by completing the square in Eq. 2 and using the Taylor series approximation $\sqrt{1+u} \approx 1 + u/2$ for $|u| \ll 1$ that

$$y_t \approx x_t'\beta + \epsilon_t \tag{3}$$

where $\epsilon_t = \eta_{Rt}\cos\theta + \eta_{It}\sin\theta \sim N(0, \sigma^2)$. This model can also be written as

$$\underset{n\times 1}{y} = \underset{n\times(q+1)}{X}\ \underset{(q+1)\times 1}{\beta} + \underset{n\times 1}{\epsilon} \tag{4}$$

where $\epsilon \sim \mathcal{N}(0, \sigma^2\Phi)$ and Φ is the temporal correlation matrix, often taken to be $\Phi = I_n$ after suitable pre-processing of the data.

The unconstrained maximum likelihood estimates of the vector of regression coefficients $\hat\beta$ and the error variance $\hat\sigma^2$ are given by

$$\begin{aligned}\hat\beta &= (X'X)^{-1}X'y,\\ \hat\sigma^2 &= (y - X\hat\beta)'(y - X\hat\beta)/n\,.\end{aligned} \tag{5}$$

To construct a generalized likelihood ratio test of the hypothesis $H_0 : C\beta = 0$ vs. $H_1 : C\beta \neq 0$, we maximize the likelihood under the constrained null hypothesis. This leads to constrained MLE's

$$\begin{aligned}\tilde\beta &= \Psi\hat\beta,\\ \tilde\sigma^2 &= (y - X\tilde\beta)'(y - X\tilde\beta)/n,\end{aligned} \tag{6}$$

where

$$\Psi = I_{q+1} - (X'X)^{-1}C'[C(X'X)^{-1}C']^{-1}C. \tag{7}$$

Then the likelihood ratio statistic for the magnitude-only model is given by

$$-2\log\lambda_M = n\log\left(\frac{\tilde\sigma^2}{\hat\sigma^2}\right). \tag{8}$$

This has an asymptotic χ^2_r distribution, where r is the full row rank of C, and is asymptotically equivalent to the usual $t-$ or F-tests associated with statistical parametric maps. For example, consider a model with β_0 representing an intercept, β_1 representing a linear drift over time, and β_2 representing a contrast effect of a stimulus. Then to test whether the coefficient for the reference function or stimulus is 0, set $C = (0, 0, 1)$, so that the hypothesis is $H_0 : \beta_2 = 0$. The LR test has an asymptotic χ^2_1 distribution and is asymptotically equivalent to the usual t tests for activation. The χ^2 representation is used for ease of comparability with the complex activation model. Alternatively, complex valued permutation resampling techniques may be used, which the author found to give similar results in the example used later.

2.2. Complex Activation

Alternatively, we can represent the observed data at time point t as a 2×1 vector instead of as a complex number

$$\begin{pmatrix} y_{Rt}\\ y_{It}\end{pmatrix} = \begin{pmatrix} x_t'\beta\cos\theta\\ x_t'\beta\sin\theta\end{pmatrix} + \begin{pmatrix}\eta_{Rt}\\ \eta_{It}\end{pmatrix}, \quad t = 1, \ldots, n\,.$$

This model can also be written as

$$\underset{2n\times 1}{y} = \underset{2n\times 2(q+1)}{\begin{pmatrix} X & 0\\ 0 & X\end{pmatrix}}\ \underset{2(q+1)\times 1}{\begin{pmatrix}\beta\cos\theta\\ \beta\sin\theta\end{pmatrix}} + \underset{2n\times 1}{\eta} \tag{9}$$

where it is specified that the observed vector of data $y = (y_R', y_I')'$ is the vector of observed real values stacked on the vector of observed imaginary values and the vector of errors $\eta = (\eta_R', \eta_I')' \sim \mathcal{N}(0, \Sigma \otimes \Phi)$ is similarly defined. Here it is assumed that $\Sigma = \sigma^2 I_2$ and $\Phi = I_n$.

As with the magnitude-only model, we can obtain unrestricted maximum likelihood estimates of the parameters as derived in the appendix to be

$$\begin{aligned}\hat\theta &= \frac{1}{2}\tan^{-1}\left[\frac{2\hat\beta_R'(X'X)\hat\beta_I}{\hat\beta_R'(X'X)\hat\beta_R - \hat\beta_I'(X'X)\hat\beta_I}\right]\\ \hat\beta &= \hat\beta_R\cos\hat\theta + \hat\beta_I\sin\hat\theta,\\ \hat\sigma^2 &= \frac{1}{2n}\left[y - \begin{pmatrix} X\hat\beta\cos\hat\theta\\ X\hat\beta\sin\hat\theta\end{pmatrix}\right]'\left[y - \begin{pmatrix} X\hat\beta\cos\hat\theta\\ X\hat\beta\sin\hat\theta\end{pmatrix}\right]\end{aligned} \tag{10}$$

where $\hat\beta_R = (X'X)^{-1}X'y_R$ and $\hat\beta_I = (X'X)^{-1}X'y_I$. Note that the estimate of the regression coefficients is a linear combination or "weighted" average of estimates from the real and imaginary parts. The regression coefficients of this model may also be estimated using principal components. Also, note that although the ML estimate of σ^2 is biased, the degree of bias is generally small ($E(\hat\sigma^2) = (2n - q - 2)/(2n) \times \sigma^2$) because n is large relative to q.

The maximum likelihood estimates under the constrained null hypothesis $H_0 : C\beta = 0$ are derived in the appendix and given by

$$\begin{aligned}\tilde\theta &= \frac{1}{2}\tan^{-1}\left[\frac{2\hat\beta_R'\Psi(X'X)\hat\beta_I}{\hat\beta_R'\Psi(X'X)\hat\beta_R - \hat\beta_I'\Psi(X'X)\hat\beta_I}\right]\\ \tilde\beta &= \Psi[\hat\beta_R\cos\tilde\theta + \hat\beta_I\sin\tilde\theta],\\ \tilde\sigma^2 &= \frac{1}{2n}\left[y - \begin{pmatrix} X\tilde\beta\cos\tilde\theta\\ X\tilde\beta\sin\tilde\theta\end{pmatrix}\right]'\left[y - \begin{pmatrix} X\tilde\beta\cos\tilde\theta\\ X\tilde\beta\sin\tilde\theta\end{pmatrix}\right]\end{aligned} \tag{11}$$

where Ψ is as defined in Eq. 7 for the magnitude-only model.

Fig. 3. Estimated reference function coefficients, β_2's.

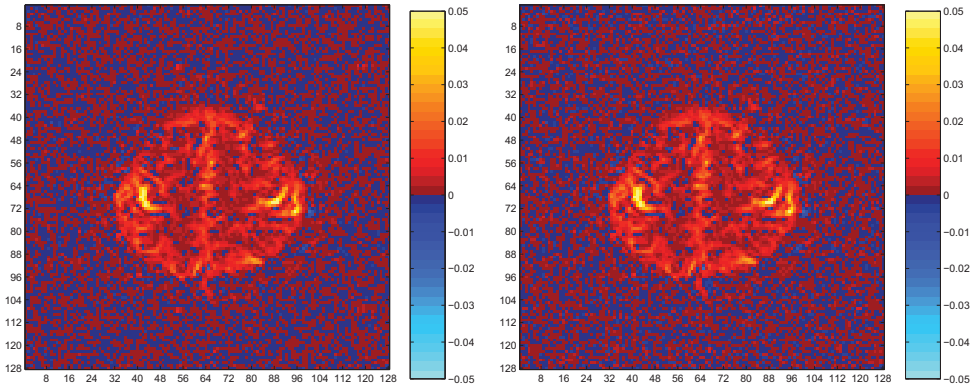

(a) Magnitude-only model

(b) Complex model

Then the generalized likelihood ratio statistic for the complex fMRI activation model is

$$-2\log\lambda_C = 2n\log\left(\frac{\tilde{\sigma}^2}{\hat{\sigma}^2}\right) . \qquad (12)$$

This statistic has an asymptotic χ^2_r distribution similar to the magnitude-only model statistic in Eq. 8 with the same caveats as mentioned previously for the magnitude-only model.

3. APPLICATION TO FMRI DATASET

A bilateral finger tapping experiment was performed in a block design with 16s off followed by eight epochs of 16s on and 16s off. Scanning was performed using a 1.5T GE Signa in which 5 axial slices of size 96×96 were acquired. In image reconstruction, the acquired data was zero filled to 128×128. After Fourier image reconstruction, each voxel has dimensions in mm of $1.5625 \times 1.5625 \times 5$, with TE$=$ 47ms. Observations were taken every TR$=$ 1000ms so that there are 272 in each voxel. Data from a single axial slice through the motor cortex was selected for analysis. Pre-processing using an ideal $0/1$ frequency filter was performed to remove respiration and low frequency physiological noise in addition to the removal of the first three points to omit machine warm-up effects.

The linear magnitude-only and nonlinear complex multiple regression models were fit to the data with an intercept, a zero mean time trend, and a ± 1 square wave reference function. Parameter estimates of the task-related activation β_2 are given in Fig. 3 for (a) the magnitude-only model and (b) the complex model. These coefficient estimates are visually very similar between the two models, but deviate slightly numerically.

As previously noted, the estimated β_2 coefficients for the complex model in Fig. 3(b) under the alternative hypothesis are a linear combination or "weighted" average between the estimated value from the real and imaginary parts. This "weighting" is displayed in Fig. 4 where the $\cos\theta$ "weights" are in Fig. 4(a), the estimated coefficient values from the real part β_{R2} are in Fig. 4(b), the $\sin\theta$ "weights" are in Fig. 4(c), and the estimated coefficient values from the real part β_{I2} are in Fig. 4(d).

Next statisticallly significant task-related activation was sought using 5% false discovery rate (FDR) and Bonferroni thresholds. These were done by applying the Benjamini-Hochberg and Bonferroni procedures to the χ^2_1 activation statistics. Images of statistically significant FDR activation are given in Fig. 5 and for statistically significant Bonferroni activation in Fig. 6 for both the magnitude-only and complex models. As previously mentioned, resampling techniques that permuted the complex valued residuals to determine false discovery rate and Bonferroni thresholded statistical parametric maps were applied and found to be virtually identical to assuming the χ^2 distribution maps.

While the activation images are similar, note that the complex model appears to have sharper or more well-defined activation regions which align better with the gray matter at which the activation is supposed to occur.

To illustrate the differences, voxels above threshold for both models are colored yellow, those only declared active for the magnitude-only model colored red and those only declared active for the complex model orange in Fig. 7.

4. CONCLUSIONS

A complex data fMRI activation model was presented as an alternative to the typical magnitude-only data model. Ac-

Fig. 4. Complex real and imaginary estimated β_2's, and trigonometric weights.

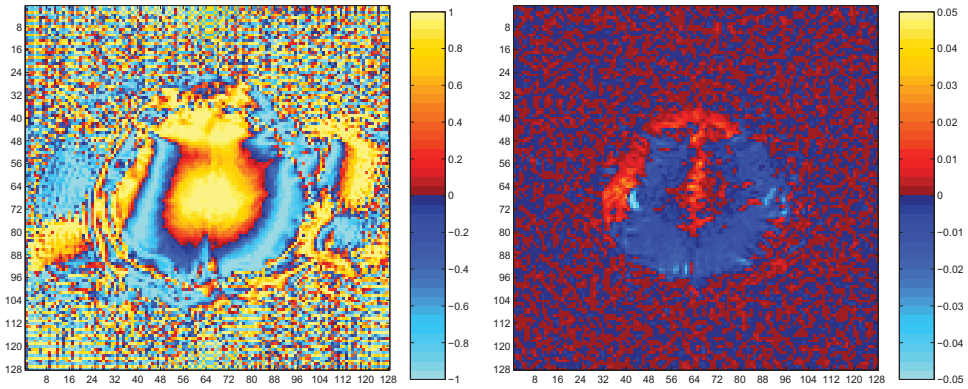

(a) real part weights, $\cos\theta$'s

(b) real part estimates, β_{R2}'s

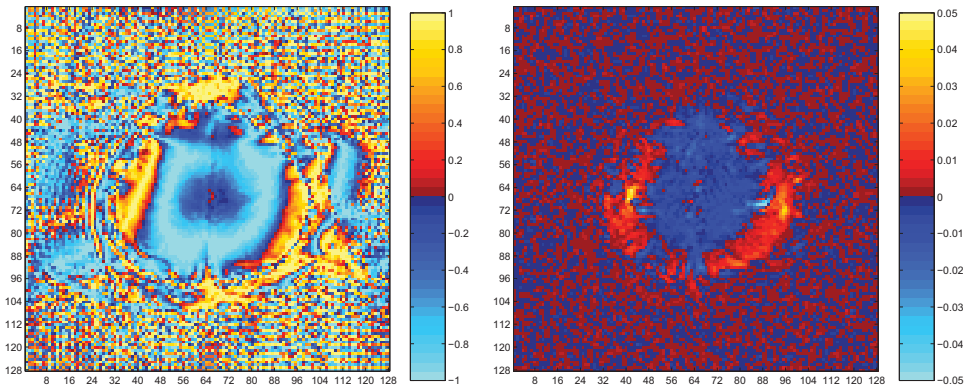

(c) imaginary part weights, $\sin\theta$'s

(d) imaginary part estimates, β_{I2}'s

tivation statistics were derived from generalized likelihood ratio tests for both models. Activation from both models were presented for real fMRI data, then simulations were performed to compare the power to detect activation regions between the two models for several signal-to-noise ratios with varying task related contrast effects.

It was found that for large signal-to-noise ratios, both models were comparable. However, for smaller signal-to-noise ratios, the complex activation model demonstrated superior power of detection over the magnitude-only activation model. This strongly indicates that modeling the complex data may become more useful as voxel sizes get smaller, since this decreases the SNR.

A. MAGNITUDE AND PHASE DISTRIBUTIONS

The distribution of the magnitude and phase can be derived as follows. Let $y_R = \rho\cos\theta + \eta_R$ and $y_I = \rho\cos\theta + \eta_I$ where η_R and η_I are normally distributed with mean zero and variance σ^2. Then, make a change of variable from (y_R, y_I) to polar coordinates $r^2 = y_R^2 + y_I^2$ and $\phi = \tan^{-1}(y_I/y_R)$ or $y_R = r\cos\phi$ and $y_I = r\sin\phi$. The Jacobian of this transformation is $J(y_R, y_I \rightarrow r, \phi) = r$. The joint distribution of r and ϕ using trigonometric identities becomes

$$p(r,\phi|\rho,\theta,\sigma^2) = \frac{r}{2\pi\sigma^2} e^{-\frac{1}{2\sigma^2}\left[r^2+\rho^2-2\rho r\cos(\phi-\theta)\right]}.$$

A.1. Magnitude Distribution

The marginal distribution of the magnitude r is found by integrating out the phase ϕ

$$p(r|\rho,\theta,\sigma^2) = \frac{r}{\sigma^2} e^{-\frac{1}{2\sigma^2}\left[r^2+\rho^2\right]} \times \int_{\phi=-\pi}^{\pi} \frac{1}{2\pi} e^{\frac{1}{\sigma^2}\rho r\cos(\phi-\theta)} d\phi$$

Fig. 5. $-2\ln\lambda$ statistics with a 5% FDR threshold

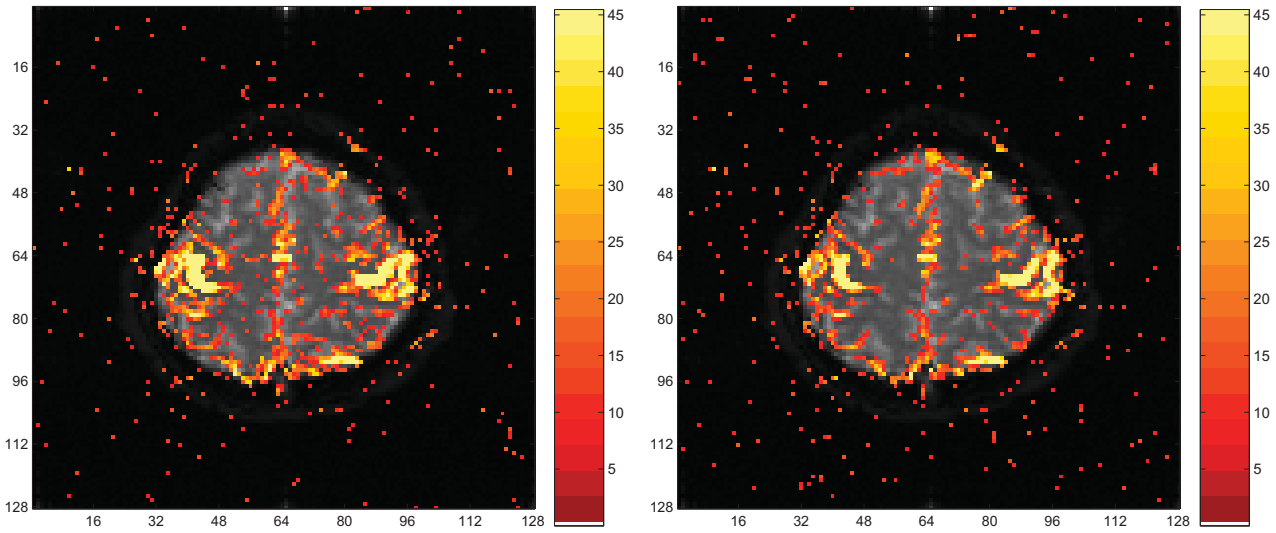

(a) Magnitude-only model

(b) Complex model

where the integral factor often denoted $I_o(r\rho/\sigma^2)$ is the zeroth order modified Bessel function of the first kind. The normal limiting distribution for large SNR or $\rho \to \infty$, is found by using the asymptotic form

$$I_o(r\rho/\sigma^2) \approx \exp(r\rho/\sigma^2)/\sqrt{(2\pi r\rho/\sigma^2)}$$

of the Bessel function [1]. Additionally, in this limit, it is assumed that the exponential form of the normal distribution drops off more rapidly compared to the variation in the ratio $\sqrt{r/\rho}$ left as a factor. The distribution of the magnitude becomes the normal distribution with mean ρ and variance σ^2. The Rayleigh limiting distribution for zero SNR or $\rho = 0$, is found by noting that $I_o(0) = 1$. The distribution of the magnitude becomes

$$p(r|\rho,\sigma^2) \quad = \quad \frac{r}{\sigma^2} e^{-\frac{r^2}{2\sigma^2}} \ .$$

A.2. Phase Distribution

The marginal distribution of the phase ϕ is found by integrating out the magnitude r

$$p(\phi|\rho,\theta,\sigma^2) \quad = \quad \frac{e^{-\frac{\rho^2}{2\sigma^2}}}{2\pi}\left[1+\frac{\rho}{\sigma}\sqrt{2\pi}\cos(\phi-\theta)\right.$$
$$\left. \times\, e^{\frac{\rho^2\cos^2(\phi-\theta)}{2\sigma^2}} \int_{z=-\infty}^{\frac{\rho\cos(\phi-\theta)}{\sigma}} \frac{e^{-z^2/2}}{\sqrt{2\pi}} dz \ .\right]$$

The normal limiting distribution for large SNR or $\rho \to \infty$, is found by multiplying through, noting that the first term is approximately zero, that the difference between ϕ and θ is small so that the cosine of their difference is approximately one, and the sine of their difference is approximately their difference. The distribution of the phase becomes the normal distribution with mean θ and variance $(\sigma/\rho)^2$.

The uniform limiting distribution for zero SNR or $\rho = 0$, is found by noting that the integral factor goes to unity. The distribution of the phase becomes uniform on $[-\pi,\pi]$. The distribution of the magnitude and phase for intermediate values of SNR can be found by numerical integration or Monte Carlo simulation. The complex model presented in this paper does not make these large SNR approximations.

B. GENERALIZED LIKELIHOOD RATIO TEST

B.1. Complex Model

In applications using multiple regression including fMRI, we often wish to test linear contrast hypothesis (for each voxel) such as

$$\begin{array}{lccclccc} H_0: & C\beta & = & \gamma & vs & H_1: & C\beta & \neq & \gamma \\ & \sigma^2 & > & 0 & & & \sigma^2 & > & 0\,, \end{array}$$

where C is an $r \times (q+1)$ matrix of full row rank and γ is an $r \times 1$ vector.

The likelihood ratio statistic is computed by maximizing the likelihood $p(y|\beta,\theta,\sigma^2,X)$ with respect to β, θ, and σ^2 under the null and alternative hypotheses. Denote the maximized values under the null hypothesis by $(\tilde{\beta},\tilde{\theta},\tilde{\sigma}^2)$ and

Fig. 6. $-2\ln\lambda$ statistics with a 5% Bonferroni threshold

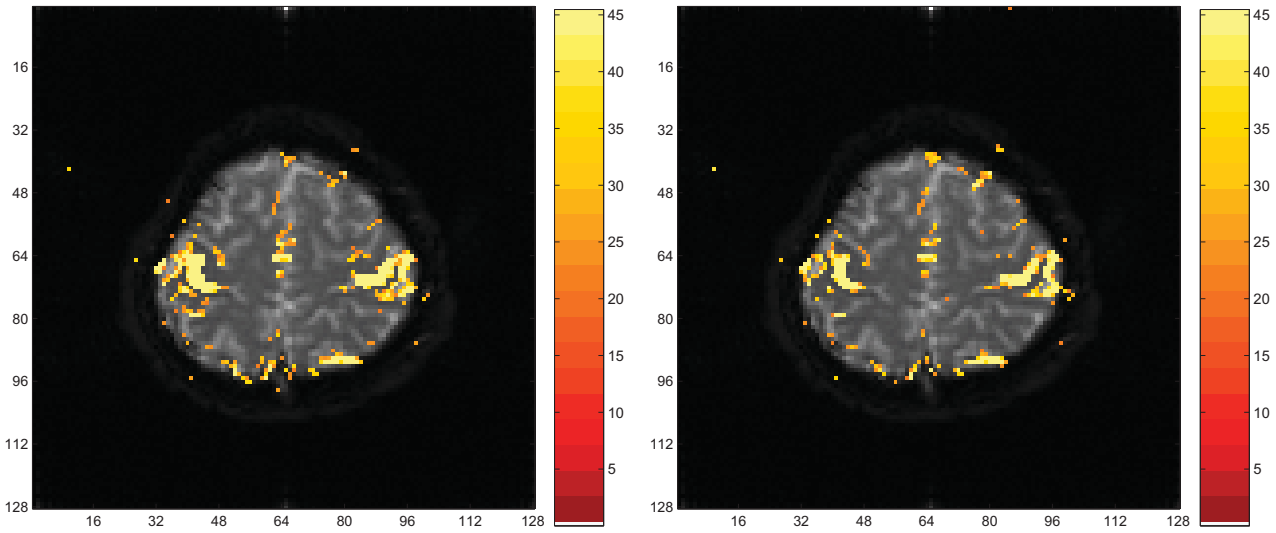

(a) Magnitude-only model

(b) Complex model

those under the alternative hypothesis as $(\hat{\beta}, \hat{\theta}, \hat{\sigma}^2)$. These maximized values are then substituted into the likelihoods and the ratio taken. With the aforementioned distributional specifications, the likelihood of the model is

$$p(y|X,\beta,\theta,\sigma^2) = (2\pi\sigma^2)^{-\frac{2n}{2}} e^{-\frac{h}{2\sigma^2}} \qquad \text{(B.1)}$$

where

$$h = \frac{1}{2n}\left[y - \begin{pmatrix} X\beta\cos\theta \\ X\beta\sin\theta \end{pmatrix}\right]' \left[y - \begin{pmatrix} X\beta\cos\theta \\ X\beta\sin\theta \end{pmatrix}\right]$$

Unrestricted MLE's

Maximizing this likelihood with respect to the parameters is the same as maximizing the logarithm of the likelihood denoted LL with respect to the parameters. In the case of β and θ it is the same as minimizing the h term in the exponent.

$$\begin{aligned}
\left.\frac{\partial h}{\partial \beta}\right| &= 2(X'X)\hat{\beta} - 2(X'X)\left[\hat{\beta}_R\cos\hat{\theta} + \hat{\beta}_I\sin\hat{\theta}\right] \\
\left.\frac{\partial h}{\partial \theta}\right| &= -2\hat{\beta}'(X'X)\left[(-\sin\hat{\theta})\hat{\beta}_R + (\cos\hat{\theta})\hat{\beta}_I\right] \\
\left.\frac{\partial LL}{\partial \sigma^2}\right| &\quad -\frac{2n}{2}\frac{1}{\hat{\sigma}^2} + \frac{\hat{h}}{2}\frac{1}{(\hat{\sigma}^2)^2}
\end{aligned}$$

where $\hat{h}$ is h with MLE's substituted in. By setting these derivatives equal to zero and solving, the MLE's under the unrestricted model given in Eq. 10 are obtained.

Restricted MLE's

Maximizing this likelihood with respect to the parameters is the same as maximizing the logarithm of the likelihood denoted LL with respect to the parameters. This is the same as minimizing the h term in the exponent with the restriction in the form of a Lagrange multiplier added to h

$$\begin{aligned}
\left.\frac{\partial h}{\partial \beta}\right| &= 2(X'X)\tilde{\beta} - 2(X'X)\left[\tilde{\beta}_R\cos\tilde{\theta} + \tilde{\beta}_I\sin\tilde{\theta}\right] \\
&\quad +2C'\tilde{\psi} \\
\left.\frac{\partial h}{\partial \theta}\right| &= -2\tilde{\beta}'(X'X)\left[(-\sin\tilde{\theta})\tilde{\beta}_R + (\cos\tilde{\theta})\tilde{\beta}_I\right] \\
\left.\frac{\partial h}{\partial \psi}\right| &= 2(C\tilde{\beta} - \gamma) \\
\left.\frac{\partial LL}{\partial \sigma^2}\right| &\quad -\frac{2n}{2}\frac{1}{\tilde{\sigma}^2} + \frac{\tilde{h}}{2}\frac{1}{(\tilde{\sigma}^2)^2}
\end{aligned}$$

where $\tilde{h}$ is h with MLE's substituted in. By setting these derivatives equal to zero and solving, the MLE's under the restricted model given in Eq. 11 are obtained.

Note that $\hat{\sigma}^2 = \hat{h}/(2n)$ and $\tilde{\sigma}^2 = \tilde{h}/(2n)$. Then the generalized likelihood ratio is

$$\lambda = \frac{p(y|\tilde{\beta},\tilde{\sigma}^2,\tilde{\theta},X)}{p(y|\hat{\beta},\hat{\sigma}^2,\hat{\theta},X)} = \frac{\left(\tilde{\sigma}^2\right)^{-2n/2} e^{-2\tilde{h}n/(2\tilde{h})}}{\left(\hat{\sigma}^2\right)^{-2n/2} e^{-2\hat{h}n/(2\hat{h})}}, \qquad \text{(B.2)}$$

and Eq. 12 for the GLRT follows.

Fig. 7. Voxels above the 5% threshold

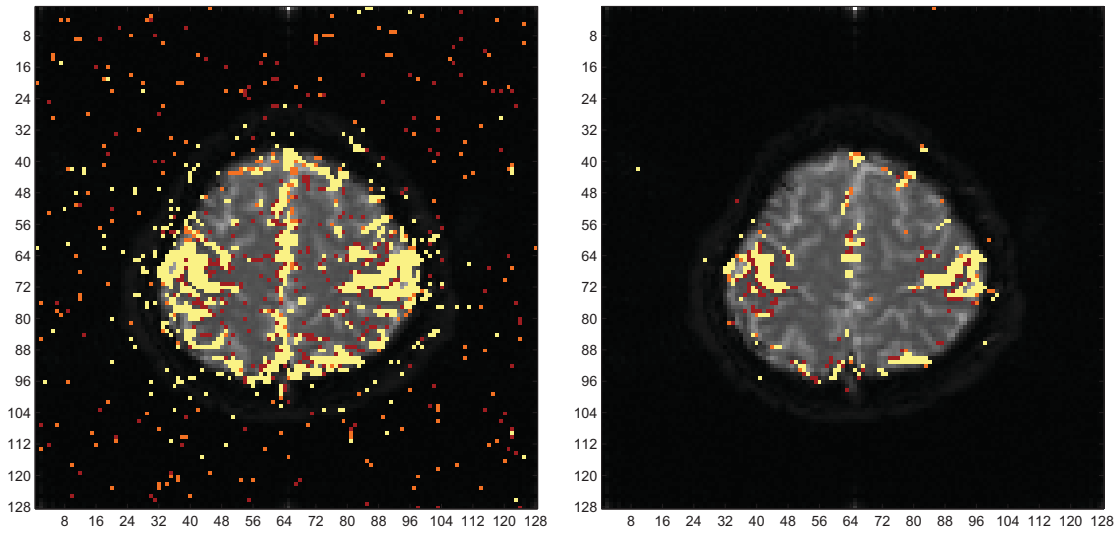

(a) FDR

(b) Bonferroni

C. REFERENCES

[1] A.H. Anderson and J.E. Kirsch. Analysis of noise in phase contrast MR imaging. *Medical Physics*, 23(6):857–869, 1996.

[2] P. Bandettini, A. Jesmanowicz, E. Wong, and J.S. Hyde. Processing strategies for time-course data sets in functional MRI of the human brain. *Magnetic Resonance in Medicine*, 30(2):161–173, 1993.

[3] Y. Benjamini and Y. Hochberg. Controlling the false discovery rate: A practical and powerful approach to multiple testing. *Journal of the Royal Statistical Society B*, 57:289–300, 1995.

[4] R.W. Cox, A. Jesmanowicz, and J.S. Hyde. Real-time functional magnetic resonance imaging. *Magnetic Resonance in Medicine*, 33(2):230–236, 1995.

[5] H. Gudbjartsson and S. Patz. The Rician distribution of noisy data. *Magnetic Resonance in Medicine*, 34(6):910–914, 1995.

[6] E.M. Haacke, R. Brown, M. Thompson, and R. Venkatesan. *Magnetic Resonance Imaging: Principles and Sequence Design*. John Wiley and Sons, New York, 1999.

[7] S. Lai and G.H. Glover. Detection of BOLD fMRI signals using complex data. *Proceedings of the ISMRM*, page 1671, 1997.

[8] B.R. Logan and D.B. Rowe. An evaluation of thresholding techniques in fMRI analysis. *Neuroimage*, 22(1):95–108, 2004.

[9] F.Y. Nan and R.D. Nowak. Generalized likelihood ratio detection for fMRI using complex data. *IEEE Transactions on Medical Imaging*, 18(4):320–329, 1999.

[10] S.O. Rice. Mathematical analysis of random noise. *Bell system Tech. J.*, 23:282, 1944. Reprinted by N. Wax, Selected papers on Noise and Stochastic Process, Dover Publication, 1954. QA273W3.

[11] D.B. Rowe. Bayesian source separation for reference function determination in fMRI. *Magnetic Resonance in Medicine*, 45(5):374–378, 2001.

[12] D.B. Rowe. *Multivariate Bayesian Statistics*. CRC Press, Boca Raton, FL, USA, 2003.

[13] L.L. Scharf and B. Friedlander. Matched subspace detectors. *IEEE Transactions on Signal Processing*, 42(8):2146–2157, 1994.